

# PIK3R1 targeting by miR-21 suppresses tumor cell migration and invasion by reducing PI3K/AKT signaling and reversing EMT, and predicts clinical outcome of breast cancer

LI-XU YAN<sup>1</sup>, YAN-HUI LIU<sup>1</sup>, JIAN-WEN XIANG<sup>2</sup>, QI-NIAN WU<sup>3</sup>, LEI-BO XU<sup>4</sup>, XIN-LAN LUO<sup>1</sup>,  
XIAO-LAN ZHU<sup>1</sup>, CHAO LIU<sup>1</sup>, FANG-PING XU<sup>1</sup>, DONG-LAN LUO<sup>1</sup>,  
PING MEI<sup>1</sup>, JIE XU<sup>1</sup>, KE-PING ZHANG<sup>1</sup> and JIE CHEN<sup>1</sup>

<sup>1</sup>Department of Pathology, Guangdong General Hospital, Guangdong Academy of Medical Science, Guangzhou, Guangdong; <sup>2</sup>Guangdong Provincial Hospital of Chinese Medicine, Guangzhou, Guangdong;

<sup>3</sup>The First Affiliated Hospital of Guangzhou Medical University, Guangzhou, Guangdong;

<sup>4</sup>Sun Yat-sen Memorial Hospital, Sun Yat-sen University, Guangzhou, Guangdong, P.R. China

Received October 18, 2015; Accepted November 22, 2015

DOI: 10.3892/ijo.2015.3287

**Abstract.** We have previously shown that dysregulation of miR-21 functioned as an oncomiR in breast cancer. The aim of the present study was to elucidate the mechanisms by which miR-21 regulate breast tumor migration and invasion. We applied pathway analysis on genome microarray data and target-predicting algorithms for miR-21 target screening, and used luciferase reporting assay to confirm the direct target. Thereafter, we investigated the function of the target gene phosphoinositide-3-kinase, regulatory subunit 1 ( $\alpha$ ) (*PIK3R1*), and detected *PIK3R1* coding protein (p85 $\alpha$ ) by immunohistochemistry and miR-21 by RT-qPCR on 320 archival paraffin-embedded tissues of breast cancer to evaluate the correlation of their expression with prognosis. First, we found that *PIK3R1* suppressed growth, invasiveness, and metastatic properties of breast cancer cells. Next, we identified the *PIK3R1* as a direct target of miR-21 and showed that it was negatively regulated by miR-21. Furthermore, we demonstrated that p85 $\alpha$  overexpression phenocopied the suppression effects of anti-miR-21 on breast cancer cell growth, migration and invasion, indicating its tumor suppressor role in breast cancer. On the contrary, *PIK3R1* knockdown abrogated anti-miR-21-induced effect on breast cancer cells. Notably, anti-miR-21 induction increased p85 $\alpha$ , accompanied by

decreased p-AKT level. Besides, anti-miR-21/*PIK3R1*-induced suppression of invasiveness in breast cancer cells was mediated by reversing epithelial-mesenchymal transition (EMT). p85 $\alpha$  downregulation was found in 25 (7.8%) of the 320 breast cancer patients, and was associated with inferior 5-year disease-free survival (DFS) and overall survival (OS). Taken together, we provide novel evidence that miR-21 knockdown suppresses cell growth, migration and invasion partly by inhibiting PI3K/AKT activation via direct targeting *PIK3R1* and reversing EMT in breast cancer. p85 $\alpha$  downregulation defined a specific subgroup of breast cancer with shorter 5-year DFS and OS, which may require more aggressive treatment.

## Introduction

Breast cancer is a heterogeneous group of malignant tumors (1). Clinicopathological surrogate definitions of subtypes have been used for a long time. However, these subtypes even have subtypes considering their distinct responses to available therapy and clinical outcomes (1,2). Although accumulating evidence supports the use of multi-gene signatures to make distinctions among breast cancer patients, the cost of these assays remains prohibitive (3). The heterogeneity in tumor cell phenotypes make breast tumor categorization a challenging task (1).

The phosphoinositide 3-kinase (PI3K) pathway provides proliferative and migratory signals and is frequently activated in human breast cancer (4-7). The PI3K family of enzymes encompasses class I, II and III, with only class I being involved in human cancer (8-11). Class IA PI3K consists of a catalytic subunit (p110 $\alpha$  as a key subunit) and a regulatory subunit (p85 $\alpha$  as a key subunit) decoded by *PIK3R1* (11-13). When lacking upstream signals, p85 stabilizes p110 and suppress its catalytic activities (14). Uchino *et al* (7) reported that *PIK3R1* was significantly downregulated in MDA-MB-231 cells and MCF-7 invasive clone compared with MCF-7 cells, thereby possibly contributing to metastasis development. Another study demonstrated that p85 $\alpha$  downregulation was an inde-

---

*Correspondence to:* Dr Li-Xu Yan or Professor Yan-Hui Liu, Department of Pathology, Guangdong General Hospital, Guangdong Academy of Medical Science, No. 106 Zhongshan Road Two, Guangzhou, Guangdong 510080, P.R. China  
E-mail: ylxys@163.com  
E-mail: yanh\_liu@163.com

**Key words:** breast cancer, miR-21, PIK3R1, migration, invasion, prognosis

pendent prognostic marker in breast cancer (15). Although the importance of the PI3K/AKT pathway in breast cancer is well known, the function of p85 $\alpha$  in breast cancer has not been widely studied.

miR-21-5p (previously named miR-21) is one of the most overexpressed miRNAs in numerous malignancies (16-19). miR-21 targets many important tumor suppressors to promote breast cancer growth, proliferation, migration and metastasis (20-22). We have previously shown that miR-21 was overexpressed in breast cancer and associated with inferior survival (23). We have reported on human genome microarray to screen potential targets of miR-21 (24).

In the present study, to elucidate the mechanisms by which miR-21 regulate breast tumor migration and invasion, we applied pathway enrichment analysis and target-predicting algorithms for the screening target of miR-21. *PIK3R1* was predicted to be a functional target of miR-21. We further investigated the regulation of *PIK3R1* coding protein p85 $\alpha$  by miR-21, the impact of changes in anti-miR-21 mediated p85 $\alpha$  expression and the clinicopathological and prognostic significance of p85 $\alpha$  in breast cancer patients.

## Materials and methods

**Cell lines.** Human breast cancer cell lines (MCF-10A, MDA-MB-231 and BT-474) were purchased from the American Type Culture Collection and cultured according to specifications. Human breast cancer cell lines (MCF-7, BT-549, T47D and SK-BR-3) were purchased from the Cell Bank of Chinese Academy of Sciences. All cells were used within 2 months after resuscitation of frozen aliquots.

**Quantification of miRNA and mRNA.** Total RNA was isolated from cells and tissues using the Total RNA Purification kit (Norgen Biotek Corp., Thorold, ON, Canada). miR-21 expression was assessed by quantitative reverse transcription-polymerase chain reaction (RT-qPCR) analysis using microRNA PCR system (Exiqon A/S) according to the manufacturer's instructions. RT-qPCR was utilized to analyze expression changes of potential miR-21 targets as previously described (23). Primers for PCR amplifications (Table I) were designed using Primer5.0 Input (version 0.4.0). Relative mRNA levels were calculated using the  $2^{-\Delta\Delta CT}$  method (25).

**Luciferase reporter assay.** The 3'-untranslated region (UTR) of *PIK3R1* containing the putative miR-21 target sites was amplified by PCR from genome DNA derived from HEK293T cells. The synthetic mutant 3'-UTR of *PIK3R1* was produced by PCR, and then the PCR products were cloned into psiCHECK-2 vector. After digestion by *XhoI* and *NotI*, the fragment containing 3'-UTR of *PIK3R1* was cloned into psiCHECK-2 vector (Promega, Madison, WI, USA). All inserts were sequenced to verify polymerase fidelity. The PCR primers are listed in Table I. HEK293T cells were cultured in 24-well plates and cotransfected with 200 ng of psiCHECK-2 vector containing 3'-UTR of *PIK3R1* and 50 nM of miRNA mimic (Exiqon A/S) per well. Transfections were performed using Lipofectamine<sup>®</sup> 2000 (Invitrogen, Carlsbad, CA, USA). The luciferase analysis was performed 48 h later using the Dual-luciferase reporter assay system (cat. no. E1910; Promega)

Table I. Sequences of RNA and DNA oligonucleotides.

Name	Sense strand/sense primer (5'-3')	Antisense strand/antisense primer (5'-3')
<b>Primers for RT-PCR</b>		
PIK3R1	TTTGCCGAGCCCTATAACT	TGCATATACTGGGTAGGCTAGT
18s rRNA	CCTGGATACCCGAGCTAGGA	GCGGCGCAATACGGAATGCCCC
<b>Primers for the 3'-UTR of <i>PIK3R1</i> cloning</b>		
PIK3R1 <i>XhoI</i> F	cgctcgagAGCGCTTACTCTTTGATCCTTCTCC	
PIK3R1 <i>NotI</i> R	CTATTAGGGTAGTGACCCATATATGGTTG	
mutPIK3R1-1	GTTTTAAATGATACCTTCAGATATTCGATCCCCACCCAGTTTTTGT	AACAAAAACTGGGGTGGGATCGAATATCTGAAGGTACATTTAAAC
mutPIK3R1-2	GTTTTGTGGGCAGTGCCTGTATTCGATCAAAAGCTGCTTTAATCAAT	ATTGATAAAAGCAGCTTTGATCGAATACAGGCACCTGCCCAACAAAAC
<b>siRNA duplexes</b>		
PIK3R1-siRNA1	CAAAGGAUUAUGCAUAAUUDtT	AAUUAUGCAUAAUCCUUUGdTdT
PIK3R1-siRNA2	CCAUAUUCACUGGUGGAAdTdT	UUCCACCAGUGAAUUAUUGGdTdT
PIK3R1-siRNA3	CUAUUGAAGCAUUUAAUUCAdTdT	UCAUUAAAUGCUUCAAUAGdTdT
Control-siRNA	UUCUCCGAACGUGUACCGUTT	ACGUGACACGUUCCGGAGAAT

RT, reverse transcription primer; F, forward primer; R, reverse primer; 3'-UTR, 3'-untranslated region.

according to the manufacturer's protocol. Firefly luciferase activity was normalized to *Renilla* luciferase activity. miRNA mimic negative control was used as the control miRNA. Experiments were carried out in triplicate.

**Cell transfection and transduction.** For transient miR-21 knockdown, the LNA-anti-miR-21 or LNA-control (Exiqon A/S, Vedbaek, Denmark) were delivered at a final concentration of 50 nM using Lipofectamine 2000 (Invitrogen). For *PIK3R1* knockdown, three siRNAs (Sigma-Aldrich, St. Louis, MO, USA) designed against *PIK3R1* (GenBank accession no. NM\_181523) were included (Table I). One control siRNA (Sigma-Aldrich) exhibiting no significant sequence similarity to human, mouse or rat gene sequence served as a negative control. Transfection was performed with Lipofectamine 2000 (Invitrogen) according to the manufacturer's instructions. For *PIK3R1* overexpression, lentivirus was produced by transfecting HEK 293T packaging cells in DMEM (HyClone, Logan, UT, USA; cat. no. SH30022.01B) with a 3-plasmid system. DNA for transfection was prepared by mixing pHelper 1.0, pHelper 2.0 and pLVX-IRES-Neo-*PIK3R1*. The empty vector pLVX-IRES-Neo was purchased from Clontech Laboratories (Mountain View, CA, USA; cat. no. 632184), and the plasmid pLVX-IRES-Neo-*PIK3R1* was generated by insertion of *PIK3R1* sequence. MDA-MB-231 cells were transduced with lentivirus in the presence of 6 µg/ml polybrene (Sigma-Aldrich) for 24 h. Cells were then selected for 7 days in 2.5 mg/ml neomycin. Overexpression of *PIK3R1* was confirmed by western blot analysis.

**Cell viability and clonogenic assays.** Cell growth and viability were measured by MTS-formazan reduction using CellTiter 96 Aqueous One Solution Cell Proliferation Assay (Promega) at 24, 48, 72 and 96 h post-transfection with a vector (empty pcDNA3.1) or *PIK3R1*. Absorbance was measured at 490 nm using a Multiskan plate reader (Thermo Labsystems, Beverly, MA, USA). Raw values were averaged, and background absorbance (medium without cells) subtracted. For this assay cells were plated at 10,000 cells/well in triplicate for each transfection condition and time-point. Raw values were averaged, and background absorbance (medium without cells) subtracted. The cellular effects of these manipulations were further investigated in MDA-MB-231 and BT-474 cells using clonogenic assays. Briefly, cells were plated on 6-well plates at 100 and 200 cells/well in triplicate and incubated at 37°C under 5% CO<sub>2</sub> for 2 days post-transfection. After 2 weeks, plates were washed, fixed in 50% methanol and stained with 0.1% crystal violet and then the number of colonies was counted.

**In vivo tumorigenicity assays.** Five-week-old female BALB/c-nude mice, provided by Shanghai Laboratory Animal Center, Chinese Academy Sciences (Shanghai, China) were used. Equivalent amounts of MDA-MB-231 cells transfected with *PIK3R1* or vector were injected subcutaneously (10<sup>7</sup> cells/tumor) into the left axilla of nude mice. Mice were weighed, and the longest and the shortest diameters of the tumor were measured every day. The tumor volume (V) was calculated according to the following equation:  $V = \frac{a \times b^2}{2}$ , where a is the longest diameter and b is the shortest diameter of the tumor (26). Thirty-six days after the initial injection,

the animals were sacrificed and tumors were extracted and weighed. The ethics guidelines for investigations in conscious animals were followed in all experiments.

**Wound healing/migration assay.** To assay the migratory response of breast cancer cells to miR-21 inhibitor or *PIK3R1* expression, the cellular effects of these manipulations were further investigated using a wound healing assay as previously described (24). Cells were allowed to reach confluence before dragging a 1-ml sterile pipette tip (Axygen Scientific, Inc., Union City, CA, USA) through the monolayer. Cells were washed with PBS to remove cellular debris and allowed to migrate for 48 h. Images were acquired at 0, 6, 24 and 48 h post-wounding with a digital camera system (Leica DFC480; Leica Microsystems, Bannockburn, IL, USA). Cell-free areas were measured with ImageJ software (National Institutes of Health, Bethesda, MD, USA) and were expressed as the percentage of migration compared to control, arbitrarily set at 100% (27). All experiments were carried out in triplicate.

**In vitro invasion assay.** Invasion of cells *in vitro* was assayed using the BD BioCoat Matrigel Invasion Chambers and Control Inserts (BD Biosciences, Bedford, MA, USA) respectively. Each well of a 24-well plate contained an insert with an 8-µm pore size polyethylene terephthalate membrane. Cells (1x10<sup>5</sup> per Transwell) were suspended in serum-free DMEM and seeded into the upper chamber. DMEM containing 2% fetal bovine serum was then added to the bottom chamber of 24-well plates to serve as a chemoattractant. After 48 h of incubation, cells on the upper surface of the filter were removed, and cells that migrated to the lower surface were fixed and stained with 1% toluidine blue. For quantification of cell invasion, 10 fields per experimental condition were randomly selected as previously described (28) and micrographed with IX71 microscope (Olympus, Tokyo, Japan). Images are representative of at least three independent experiments.

**Western blots.** Cells were harvested and lysed in radio-immunoprecipitation buffer (Upstate Biotechnology, Inc., Lake Placid, NY, USA). Antibodies used for immunoblot analysis were p85α 1:1,000 (Cell Signaling Technology, 13666), p110α 1:1,000 (Cell Signaling Technology, 42336), p-AKT (Ser473) 1:2,000 (Cell Signaling Technology, 4060), AKT 1:1,000 (Cell Signaling Technology, 9272), E-cadherin 1:1,000 (Cell Signaling Technology, 3195), N-cadherin 1:1,000 (Cell Signaling Technology, 13116), vimentin 1:1,000 (Abcam, 92547), FSP1 1:1,000 (Cell Signaling Technology, 13018), snail 1:1,000 (Cell Signaling Technology, 3879) and slug 1:1,000 (Cell Signaling Technology, 9585). GAPDH 1:3,000 (Santa Cruz Biotechnology, sc-32233) or β-actin 1:1,000 (Cell Signaling Technology, 8457) were used as loading controls. All bands were detected using a SuperSignal West Pico Chemiluminescent Substrate (Pierce, Rockford, IL, USA).

**Tissue specimens.** Eligible patients were women with invasive breast cancer, no special type; operable; no previous chemotherapy; adequate formalin-fixed paraffin-embedded (FFPE) tumor specimens from the pre-treatment biopsy or surgery sample for representation in tissue microarrays (TMAs); outcome data available. Patients with distant metastases or a

history of a previous or concomitant malignancy were excluded. The archived FFPE tissues were obtained from the Department of Pathology, Guangdong General Hospital between 2009 and 2012. A consensus diagnosis of invasive breast cancer was confirmed by two expert pathologists according to the fourth edition of the World Health Organization (WHO) classification of tumors of the breast, published in 2012 (29). The surrogate definition of intrinsic subtypes of breast cancer was according to the St Gallen International Expert Consensus 2013 (3). The clinicopathological characteristics of the patients are summarized in Table II. Median follow-up time was 36 months (range, 5-68 months). The Research Ethics Committee of Guangdong General Hospital and Guangdong Academy of Medical Science reviewed and approved the study (no. GDREC2012022H) according to the principles expressed in the Declaration of Helsinki. The Research Ethics Committee specifically waived the need for informed consent for this retrospective study.

**TMA construction and immunohistochemistry (IHC).** TMAs that contained three representative 2.0-mm cores from each tumor of the cases were prepared with a tissue microarrayer (Beecher Instruments, Silver Spring, MD, USA). Immunohistochemical staining was performed using Real EnVision kit (K5007; Dako, Carpinteria, CA, USA) on an automated immunostaining instrument (Leica Bond-Max; Leica Microsystems GmbH, Wetzlar, Germany) according to the manufacturer's instructions. Internal control cores were present in each TMA. Sections were subjected to staining protocols with the anti-PI3 kinase p85 $\alpha$  antibody (EP380Y) (Abcam; cat. no. ab40755). A negative control was performed in all cases by omitting the primary antibody, which in all instances resulted in negative immunoreactivity. Positive immunohistochemical staining was defined as a brown cytoplasmic staining for p85 $\alpha$ . A semi-quantitative intensity scale ranging from 0 (no staining) to 3+ (the most intense staining) was used by comparing neoplastic cells to adjacent breast cells belonging to normal terminal duct lobular units as previously described (15). p85 $\alpha$  downregulation was defined by an IHC score 0, and p85 $\alpha$  overexpression by an IHC score 1+ to 3+ (15). The localization and intensity of staining were assessed by two independent pathologists. Hormonal receptors were evaluated with the 1D5 antibody for the estrogen receptor (ER; Dako) and antibody PGR-1A6 for the progesterone receptor (PR; Dako). The human epidermal growth factor receptor 2 (HER2/neu) was detected with CB11 (Dako). Hormonal receptors and gene copy number of HER2 were assessed by IHC staining on 4- $\mu$ m thick tumor sections from FFPE blocks.

**Fluorescein in situ hybridization (FISH).** HER2 amplification status was detected by PathVysion kit (Abbott) according to the manufacturer's instructions. HER2 was defined as amplified when the FISH ratio was 2 or greater.

**Statistical analysis.** Statistical analysis was prepared using the Statistical Package of MedCalc statistical software (version 12.7.4; MedCalc Software, Mariakerke, Belgium) and Social Sciences (version 20.0; SPSS, Inc., Chicago, IL, USA). The receiver operating characteristic curves were constructed to estimate the optimal cut-off points for of p85 $\alpha$  protein and miR-21 as the predictors for disease-free survival (DFS) and

Table II. Patient clinicopathological characteristics.

Characteristics	Patients (N=320)	
	No. of patients	%
Median age (range), years	50 (25-91)	
Clinical stage at diagnosis		
I	109	34.1
II	144	45.0
III	67	20.9
Tumor stage (size cm)		
T1 ( $\leq$ 2.0)	157	49.1
T2 ( $>$ 2.0 to $\leq$ 5.0)	131	40.9
T3 ( $>$ 5.0)	26	8.1
T4 <sup>a</sup>	6	1.9
Nodal stage		
N0 (node negative)	178	55.6
N1 (1-3 positive nodes)	83	25.9
N2 (4-9 positive nodes)	36	11.3
N3 ( $\geq$ 10 positive nodes)	23	7.2
Histological grade		
Grade 1	16	5.0
Grade 2	176	55.0
Grade 3	128	40.0
Subtypes of breast cancer		
Luminal A-like	71	22.2
Luminal B-like	186	58.1
HER2 positive (non-luminal)	27	8.4
Triple negative (ductal)	31	9.7
Not known	5	1.6
ER status		
Negative	66	20.6
Positive	254	79.4
PR status		
Negative	78	24.4
Positive	242	75.6
HER2 status		
Negative	238	74.4
Positive	69	21.6
Not known	13	4.1
Surgery		
Mastectomy	281	87.8
Breast conservation	39	12.2
Chemotherapy		
Neoadjuvant chemotherapy	70	21.9
Adjuvant chemotherapy	165	51.6
Not given	85	26.6
Targeted therapy		
Herceptin	12	3.8
No herceptin	308	96.3

ER, estrogen receptor; PR, progesterone receptor; HER2, human epidermal growth factor receptor 2. <sup>a</sup>T4, tumor of any size with direct extension to the chest wall and/or to the skin.

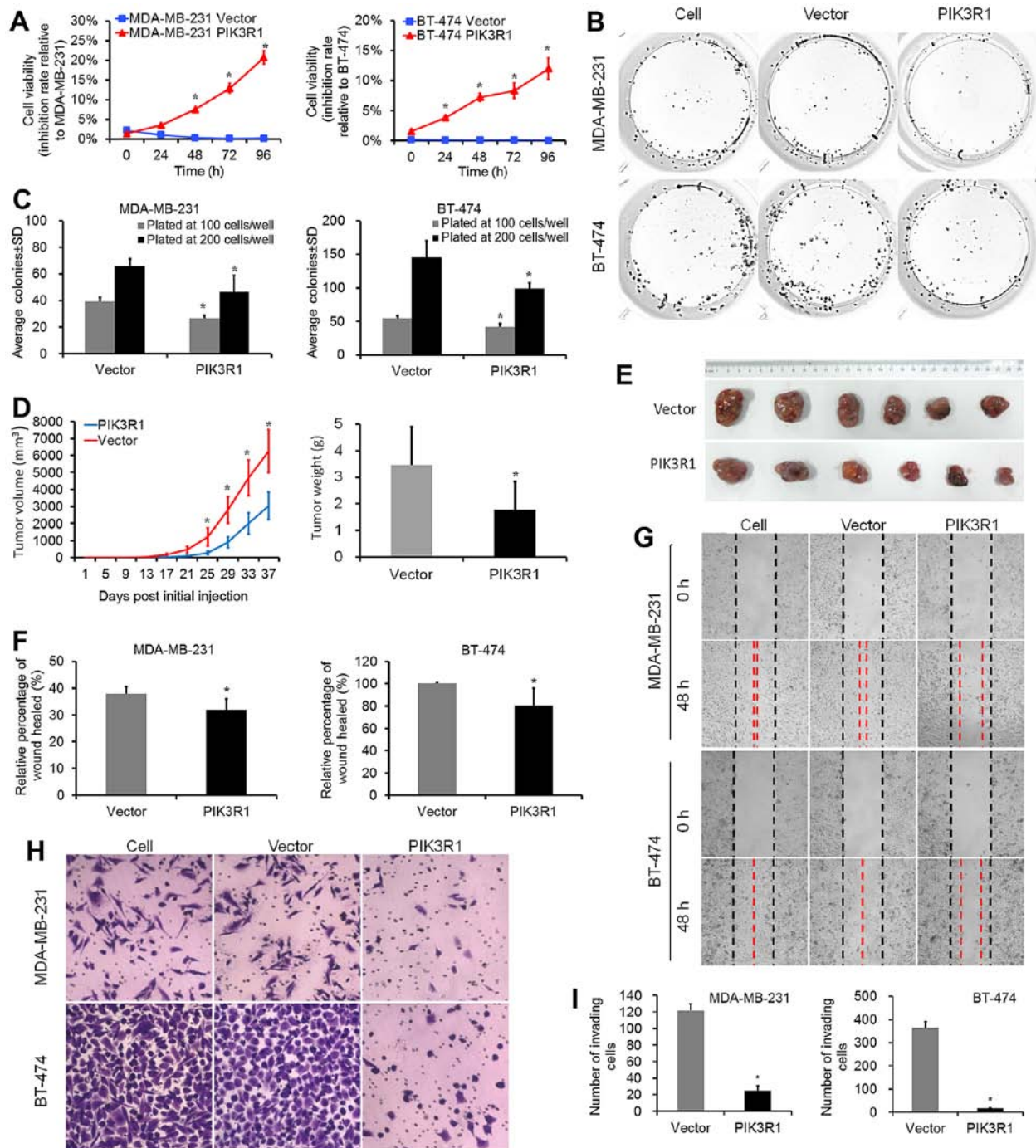


Figure 1. PIK3R1 overexpression reduces breast cancer cell proliferation, clonogenicity, migration and invasion. (A) MTS assays showed that at 48, 72 and 96 h, the PIK3R1 overexpressing lines showed significantly reduced levels of proliferation as compared to control lines. (B) Clonogenic assays performed with MDA-MB-231 and BT-474 cells plated at 200 cells/well. (C) Clonogenic assay showed that PIK3R1 overexpression resulted in a decrease in colony number as compared to control lines. (D) Growth curves for PIK3R1 group (n=6) vs. control (n=6) group in an *in vivo* proliferation assay. Tumors were weighed after animals were sacrificed at 36 days post-tumor cell injection. (E) Tumors extracted from PIK3R1 group and control group. (F and G) Migration assays performed with PIK3R1 overexpression and control cells. (H and I) Invasion assays in the control and PIK3R1-transfected cells. Data represent mean  $\pm$  SD. \*P<0.05; \*\*P<0.01.

overall survival (OS). Pearson's Chi-square test and Spearman rank correlation analysis were used to determine association and correlation between variables. Survival analyses were plotted using Kaplan-Meier curves and compared using the log-rank test. Univariate and multivariate survival analyses were analyzed by Cox proportional hazards regression models. The results were considered statistically significant when two-sided P<0.05.

## Results

*PIK3R1* suppresses growth, invasiveness and metastatic properties of breast cancer cells. *PIK3R1* overexpression significantly reduced proliferation and colony formation capabilities in MDA-MB-231 and BT-474 cell lines as compared to control cells (Fig. 1A-C). *In vivo* study showed that at the 36th day, the average tumor volume in the *PIK3R1* group

Table III. Top three signaling pathways for *PIK3R1* in breast cancer cells.

Pathway analysis	Pathway name	Total	P-value	Q-value	Gene
KEGG	Regulation of actin cytoskeleton	7	0.012	0.002	<i>LIMK1, SLC9A1, GNG12, WASF2, PIK3R1, ARPC4, ACTN4</i>
	Insulin signaling pathway	5	0.024	0.003	<i>FLOT2, PRKCI, PPP1R3C, PIK3R1, PHKA2</i>
	Apoptosis	4	0.025	0.003	<i>APAF1, TRAF2, NFKB2, PIK3R1</i>
GenMAPP	Lipid binding	9	0.001	<0.001	<i>PRKCI, ANXA6, SCP2, STARD3, WDFY1, ANXA2, PREX1, PIK3R1, BPI</i>
	Kinase activity	5	0.044	0.005	<i>ADCK4, GALK1, AK3, CARKL, PIK3R1,</i>
	Apoptosis	4	0.023	0.003	<i>APAF1, IRF1, TRAF2, PIK3R1</i>
BioCarta	Role of PI3K subunit p85 in regulation of actin organization and cell migration	3	0.001	<0.001	<i>ACTR2, PIK3R1, ARPC4</i>
	EGF signaling pathway	3	0.004	0.001	<i>STAT3, PIK3R1, MEF2D</i>
	PDGF signaling pathway	3	0.004	0.001	<i>STAT3, PIK3R1, MEF2D</i>
	Signaling of hepatocyte growth factor receptor	3	0.009	0.002	<i>STAT3, PIK3R1, MEF2D</i>
	Mechanism of gene regulation by peroxisome proliferators via PPAR $\alpha$	3	0.020	0.003	<i>PPARBP, EHHADH, PIK3R1</i>

(3040 $\pm$ 812 mm<sup>3</sup>, mean  $\pm$  SD) was significantly smaller than that in the control group (Fig. 1D and E; 6258 $\pm$ 1263 mm<sup>3</sup>, P=0.008). Moreover, the average tumor weight in the *PIK3R1* group (1.78 $\pm$ 1.05 g) was lower than that in the control group (Fig. 1D; 3.46 $\pm$ 1.43 g, P=0.046). *PIK3R1* overexpression reduced the average percentage of wound healed in both MDA-MB-231 and BT-474 cell lines as measured at 48 h (Fig. 1F and G; P<0.001 for both lines as compared to control lines). We used the BD Biocoat Matrigel Invasion Assay to test the invasive capabilities of MDA-MB-231 and BT-474 cells expressing *PIK3R1*. For the 2 lines, *PIK3R1* strongly reduced the number of invaded cells vs. controls, with the lowest percent invasion in PIK3R1-BT-474 lines (Fig. 1H and I; 4.4%). These data suggest that *PIK3R1* plays an important role in the suppression of cell proliferation, migration and invasion of breast cancer cells.

*PIK3R1* is a direct target of miR-21. We have previously identified miR-21 as an oncomiR in breast cancer and have used human genome microarray to identify potential targets of miR-21 (24). In the present study, to biologically and metabolically interpret the array data, we applied pathway enrichment analysis with KEGG (<http://www.genome.jp/kegg/>), GenMAPP (<http://www.genmapp.org/>), and BioCarta (<http://www.biocarta.com/>), and identified a set of interesting genes, including *PIK3R1*, *NFKB2*, *STAT3* and *AK3* (Table III). To narrow down candidate target genes, we applied mRNA target-predicting algorithms (TargetScan, picTar, miRDB, PITA and microRNA.org) based on the presence of binding sites in the 3'-UTR. All the five algorithms identified *PIK3R1* as the potential target of miR-21.

Interestingly, p85 $\alpha$  has previously been shown to exert tumor suppressor properties through negative regulation of growth factor signaling (30). *PIK3R1* expression was signifi-

cantly decreased by 18% in breast cancer tissues (31) and cell lines (7), and was associated with decreased survival in breast cancer patients (15). Therefore, we conducted analyses to determine whether miR-21 might target *PIK3R1*. First, we examined miR-21 and *PIK3R1* mRNA in a range of metastatic (BT-474, MDA-MB-231 and BT-549), and non-metastatic (MCF-7, SK-BR-3 and T-47D) human breast cancer cell lines and breast epithelial cell line MCF-10A. All breast cancer lines tested, except SK-BR-3 and T-47D, exhibited elevated levels of miR-21 compared to MCF-10A cells, with corresponding reductions in *PIK3R1* levels (Fig. 1A). Next, to establish a direct relationship between miR-21 and the predicted target gene, a luciferase construct containing the 3'-UTR of *PIK3R1* was transfected with a miR-21 mimic, or a miRNA-negative control mimic (Fig. 1B); a 44% reduction in luciferase activity was observed only with the miR-21 mimic (Fig. 1C). To further show that miR-21 interacts directly with two seed-binding regions within the 3'-UTR of *PIK3R1*, two point mutations were generated in each seed-binding region and were denoted as Mut845 and Mut1091 (Fig. 1B). Although a significant reduction in luciferase activity was observed for the WT construct, high luciferase activity was maintained in all of the mutants (Fig. 1C), thereby supporting the direct interaction between miR-21 and these two targeted regions within the *PIK3R1* 3'-UTR.

*AntimiR-21 suppresses tumor growth, invasiveness and metastasis by targeting PIK3R1 via PI3K/AKT signaling.* We previously found that LNA-antimiR-21 suppressed breast cancer cell growth and migration *in vitro* (24). In order to determine whether antimiR-21-induced suppression of growth, invasiveness and metastases of breast cancer cells are indeed executed via *PIK3R1*, we utilized MDA-MB-231 and BT-474 cells, which express high levels of endogenous miR-21, and

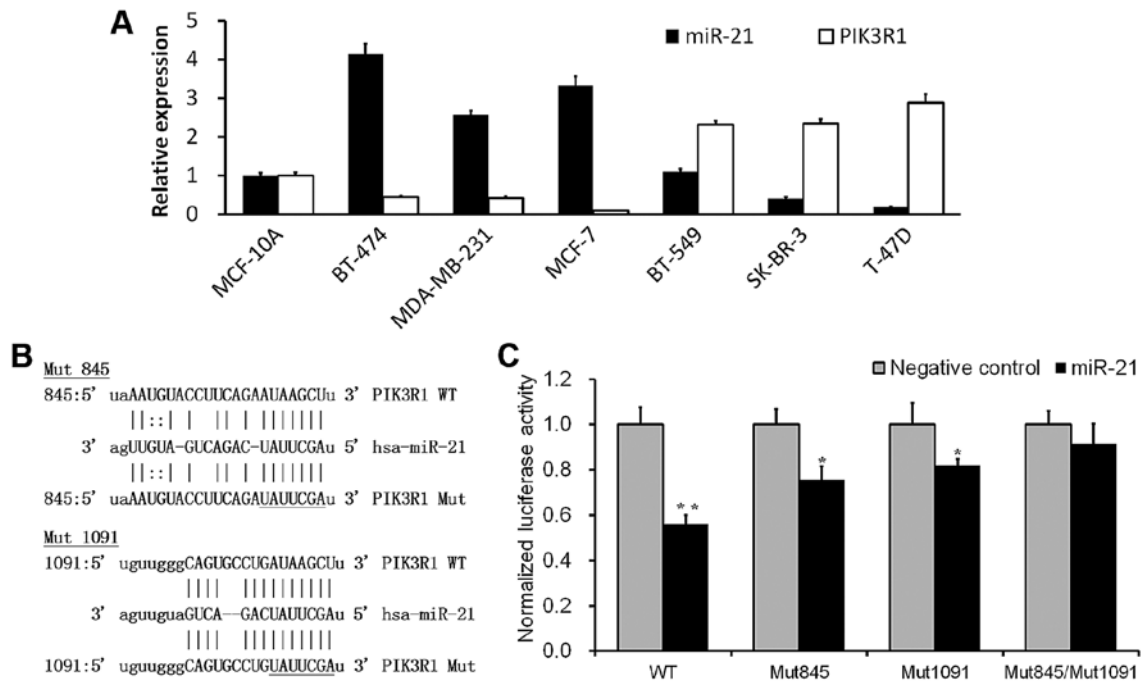


Figure 2. miR-21 targets the 3'-UTR of *PIK3R1*. (A) miR-21 and *PIK3R1* expression levels in breast cancer cell lines relative to MCF-10A cells. (B) Two miR-21-targeted regions within the 3'-UTR of *PIK3R1* were identified and then mutated using two point mutations each. (C) Luciferase activity was measured for the WT 3'-UTR of *PIK3R1* and the mutants after miR-21 transfection. Data represent mean  $\pm$  SD. \*P<0.05; \*\*P<0.01.

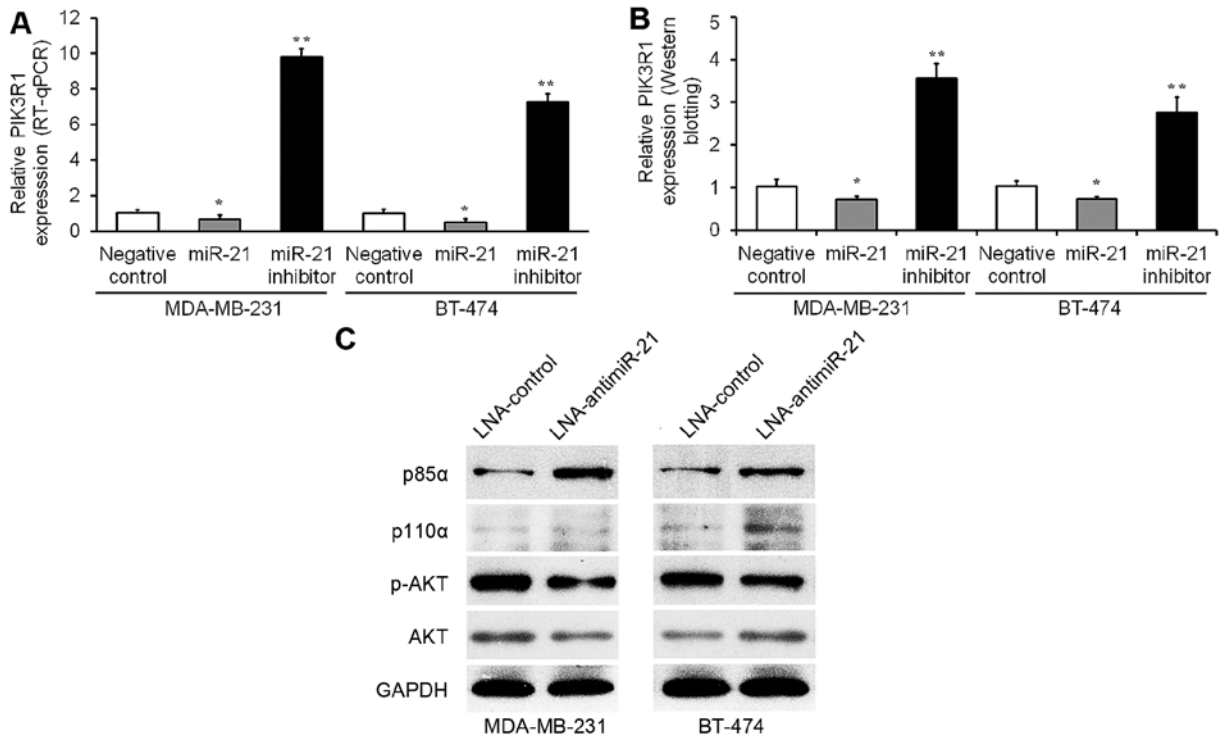


Figure 3. The miR-21-dependent proto-oncogene PI3K/AKT pathway is active in breast cancer cell lines. *PIK3R1* expression was measured by (A) RT-qPCR and (B) western blot analysis in breast cancer cell lines with upregulated miR-21, miR-21 knockdown or control. (C) Immunoblots using the stated antibodies of lysates from breast cancer cells transfected with LNA-antimiR-21 or LNA-control. GAPDH served as the loading control. Data represent mean  $\pm$  SD. \*P<0.05; \*\*P<0.01.

transfected them with LNA-antimiR-21. Indeed, inhibition of miR-21 in breast cancer cells resulted in a 7- to 9-fold increase in *PIK3R1* mRNA levels (Fig. 3A) and an approximate 3-fold increase in protein (p85 $\alpha$ ) levels (Fig. 3B). Furthermore, over-

expression of miR-21 resulted in a 30-50% reduction in *PIK3R1* mRNA levels (Fig. 3A) and an approximate 30% reduction in protein levels (Fig. 3B) in both MDA-MB-231 and BT-474 cells. Concomitant with the increase in p85 $\alpha$ , a decrease in



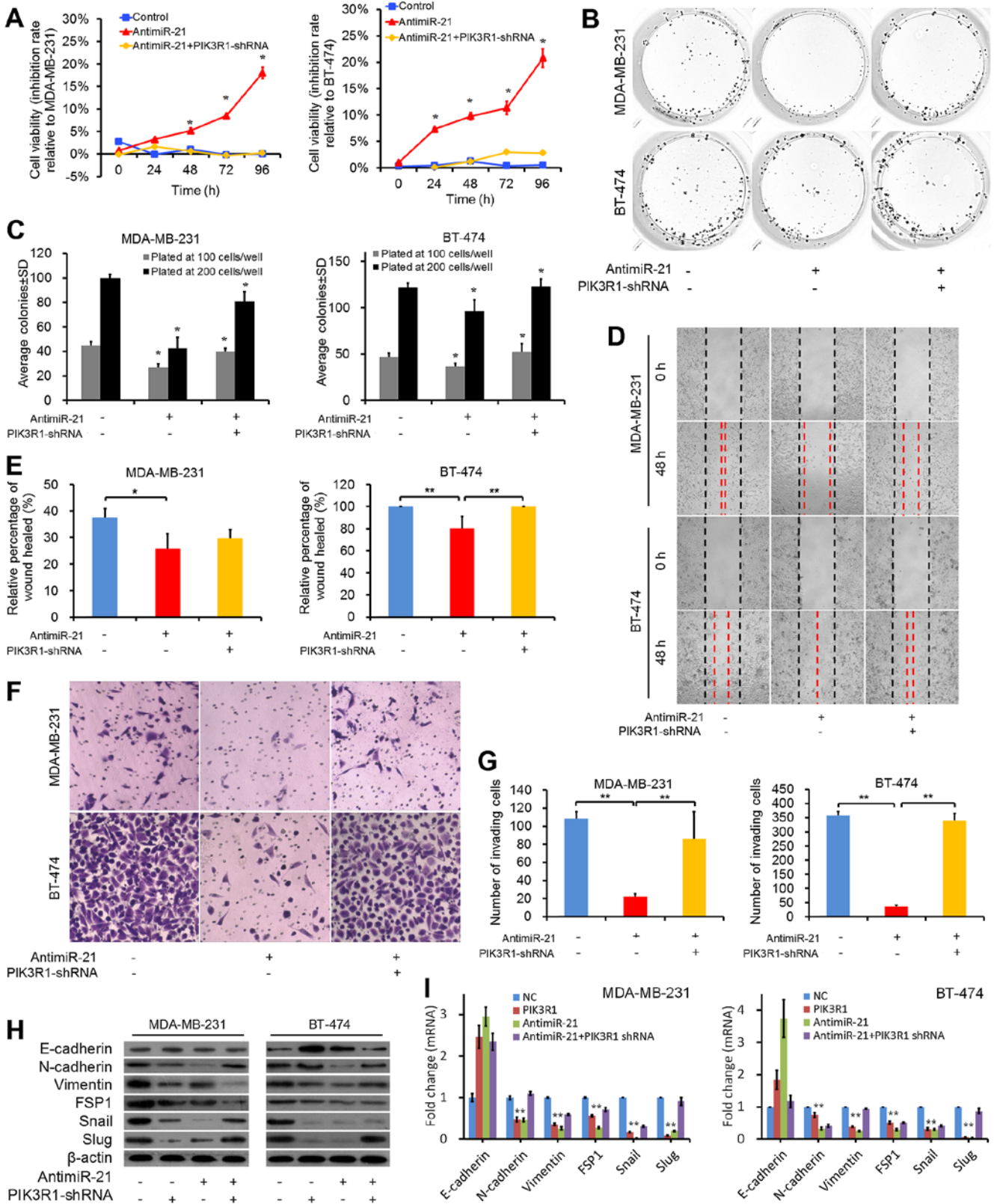


Figure 4. AntimiR-21-induced suppression of proliferation, clonogenicity, invasiveness, and metastatic properties of breast cancer cells is mediated by direct repression of *PIK3R1*. (A) MTS assays were conducted on breast cancer cells after transfection with anti-miR-21 (50 nmol/l), anti-miR-21 + *PIK3R1*-shRNA or control. At 48, 72 and 96 h, the anti-miR-21 lines showed significantly reduced levels of proliferation as compared to control lines. *PIK3R1*-shRNA reversed the effect of anti-miR-21 on cells. (B) Representative images depicting clonogenic assays performed with cells plated at 200 cells/well. (C) In MDA-MB-231 and BT-474 lines, anti-miR-21 resulted in a decrease in colony number as compared to control lines. *PIK3R1*-shRNA reversed the effect of anti-miR-21 on cells. (D) Representative images depicting cell migration assays. (E) Cell migration was quantitated as percentage of wound-healed area from corresponding control and transfected cells. (F) Invasion assays in these control and transfected cells. (G) For each cell line, anti-miR-21 resulted in reduced invasion as compared to controls. *PIK3R1* knockdown reversed the effect of anti-miR-21 on cell migration in both cell lines. (H) MDA-MB-231 and BT-474 lines were transfected with *PIK3R1*, anti-miR-21, anti-miR-21 + *PIK3R1*-shRNA or control, followed by western blot analysis of the indicated EMT-related proteins. Relative E-cadherin, N-cadherin, vimentin, FSP1, snail and slug levels were normalized to the  $\beta$ -actin level. (I) Breast cancer lines were transfected with *PIK3R1*, anti-miR-21, anti-miR-21 + *PIK3R1*-shRNA or control, followed by RT-qPCR analysis of the indicated EMT-related mRNAs. Data represent mean  $\pm$  SD. \* $P < 0.05$ ; \*\* $P < 0.01$ .



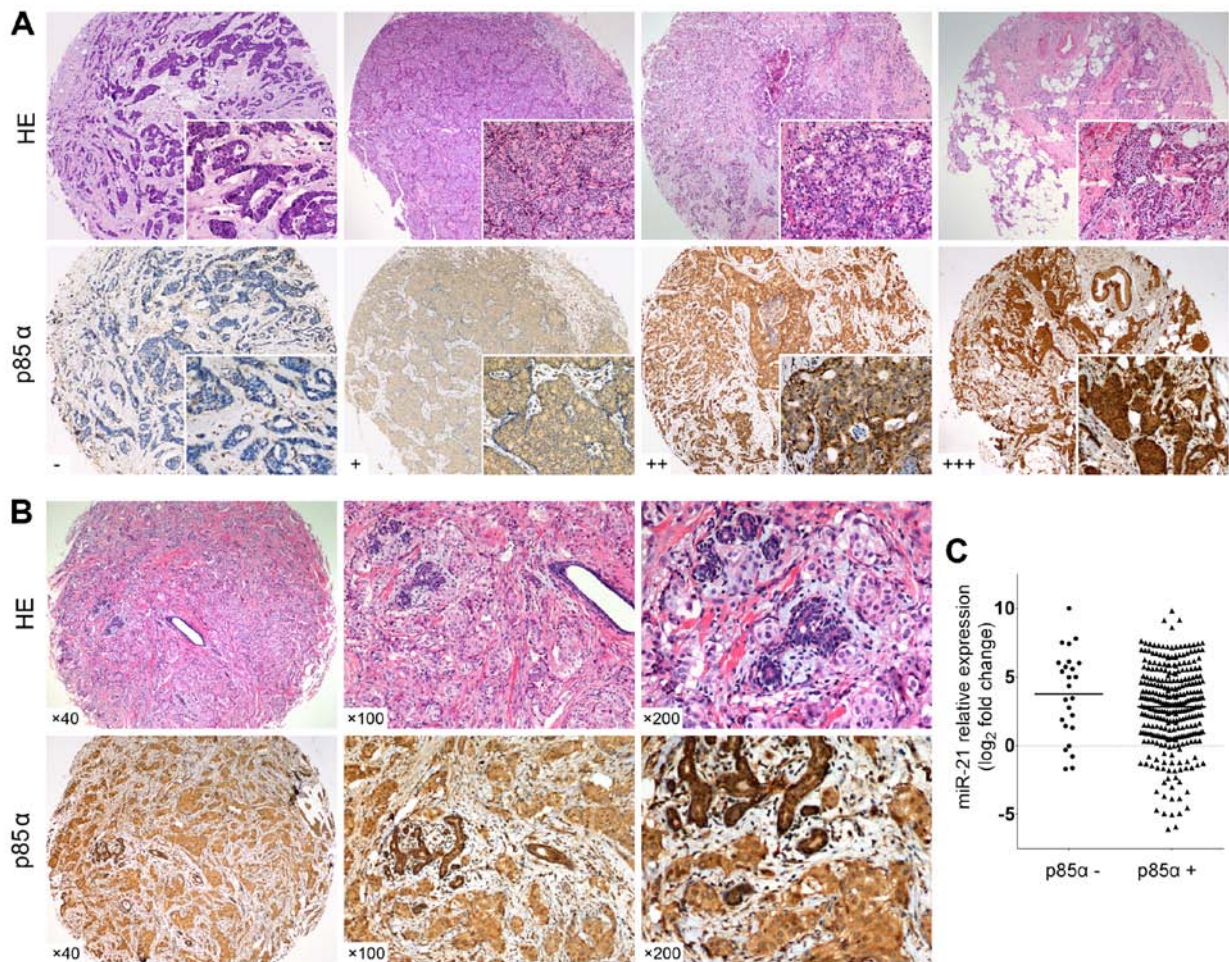


Figure 5. Tissue microarray based immunohistochemical analysis of p85 $\alpha$  expression in breast cancer tissues. (A) Representative sections for staining intensity -, +, ++ and +++ of p85 $\alpha$  protein are shown. Images were taken at x40 and x200 magnification. (B) Breast cancer cells exhibited a weaker p85 $\alpha$  expression (staining intensity ++) than surrounding residual normal duct lobular units (staining intensity +++). (C) miR-21 expression in p85 $\alpha$  overexpression (p85 $\alpha$  +) and p85 $\alpha$  downregulation (p85 $\alpha$  -) breast cancers was analyzed by RT-qPCR.

PI3K pathway activation was observed, as evidenced by decreased p-AKT expression (Fig. 3C). These results suggest that miR-21-dependent proto-oncogene PI3K/AKT pathway is active in breast cancer cell lines.

Moreover, *PIK3R1* overexpression phenocopied the suppression effects of LNA-antimiR-21 on cell proliferation and colony formation capabilities. Notably, *PIK3R1* knockdown abrogated LNA-antimiR-21-induced suppression of cell proliferation and colony formation capabilities (Fig. 4A-C). LNA-antimiR-21 reduced the average percentage of wound healed in both cell lines as measured at 48 h ( $P < 0.001$ ). In BT-474 cells, *PIK3R1* knockdown significantly abrogated LNA-antimiR-21-mediated cell migration ( $P = 0.007$ ). Although not in a statistically significant manner, *PIK3R1* knockdown also abrogated LNA-antimiR-21-mediated cell migration in MDA-MB-231 cells (Fig. 4D and E). We used the BD Biocoat Matrigel Invasion Assay to test the invasive capability of MDA-MB-231 and BT-474 cells lacking miR-21. For these lines, LNA-antimiR-21 strongly reduced the number of invaded cells vs. controls, with the lowest percent invasion in the *PIK3R1*-BT-474 line (Fig. 4F and G; 4.4%). Furthermore, *PIK3R1* knockdown significantly abrogated LNA-antimiR-21-mediated cell invasion in MDA-MB-231 ( $P = 0.004$ ) and BT-474

lines ( $P < 0.001$ ). Together, these data support the hypothesis that miR-21 by targeting *PIK3R1* promotes breast cancer cell growth, invasion and migration.

*AntimiR-21 reverses the epithelial-mesenchymal transition (EMT) target PIK3R1 suppression of invasiveness in breast cancer.* To determine whether antimiR-21/*PIK3R1*-induced suppression of invasiveness in breast cancer cells is mediated by reversing EMT, we transfected the MDA-MB-231 and BT-474 cell lines, which exhibit a mesenchymal phenotype, with antimiR-21 or *PIK3R1*. Transfection of breast cancer cells with antimiR-21 or *PIK3R1* resulted in reversal of EMT, as evidenced by repression of the mesenchymal markers N-cadherin, vimentin, FSP1, snail and slug and induction of the epithelial marker E-cadherin. Furthermore, *PIK3R1* shRNA reversed the effect of antimiR-21 or *PIK3R1* on EMT (Fig. 4H and I).

*p85α downregulation in patient tumor specimens.* To establish the relevance of our findings in the patient tumors, we analyzed the expression of miR-21 by RT-qPCR and p85 $\alpha$  by IHC in 320 primary human invasive breast cancers, and the adjacent non-tumor-affected epidermis. Alteration of p85 $\alpha$  was also

Table IV. Correlation between p85 $\alpha$  protein expression and clinicopathological parameters of breast cancer patients.

Characteristics	p85 $\alpha$			miR-21		
	Overexpression (n=295) N (%)	Downregulation (n=25) N (%)	P-value	Low (n=201) N (%)	High (n=119) N (%)	P-value
Clinical stage						
I	100 (34)	9 (36)	0.860	73 (36)	36 (30)	<i>0.016</i>
II	134 (45)	10 (40)		96 (48)	48 (40)	
III	61 (21)	6 (24)		32 (16)	35 (29)	
Tumor size (cm)						
≤2	144 (49)	13 (52)	0.760	97 (48)	66 (55)	0.213
>2	151 (51)	12 (48)		104 (52)	53 (45)	
Node						
Negative	164 (56)	14 (56)	0.969	118 (59)	60 (50)	0.149
Positive	131 (44)	11 (44)		83 (41)	59 (50)	
Histological grade						
1	13 (4)	3 (12)	0.245	13 (6)	3 (3)	0.110
2	163 (55)	13 (52)		103 (51)	73 (61)	
3	119 (40)	9 (36)		85 (42)	43 (36)	
Subtypes of breast cancer						
Luminal A-like	63 (21)	8 (32)	0.095 <sup>a</sup>	43 (21)	28 (23)	0.095 <sup>a</sup>
Luminal B-like	170 (58)	16 (64)		113 (56)	73 (61)	
HER2 positive	27 (9)	0 (0)		18 (9)	9 (8)	
Triple negative	30 (10)	1 (4)		24 (12)	7 (6)	
Not known	5 (2)	0 (0)		3 (2)	2 (2)	
ER						
Negative	64 (22)	2 (8)	0.104	47 (23)	19 (16)	0.113
Positive	231 (78)	23 (92)		154 (77)	100 (84)	
PR						
Negative	76 (26)	2 (8)	0.047	55 (27)	23 (19)	0.106
Positive	219 (74)	23 (92)		146 (73)	96 (81)	
HER2						
Negative	218 (74)	20 (80)	0.467 <sup>b</sup>	154 (77)	84 (71)	0.591 <sup>b</sup>
Positive	65 (22)	4 (16)		42 (21)	27 (23)	
Not known	12 (4)	1 (4)		5 (2)	8 (7)	

P-values were derived from Pearson's Chi-square test. Italics indicate significance. <sup>a</sup>P-value Luminal A and B vs. <sup>b</sup>P-value HER2-negative vs. HER2-positive and triple negative.

verified at the protein level by IHC staining on TMAs. Positive staining of p85 $\alpha$  was found in the cytoplasm (Fig. 5A). Tumor cells showed p85 $\alpha$  moderate expression, while residual normal mammary epithelial cells presented strong IHC staining intensity (Fig. 5B).

Staining scores and log<sub>2</sub> of C<sub>T</sub> values were analyzed using MedCalc statistical software to determine the optimal survival cut-off points for dichotomizing expression of p85 $\alpha$  protein and miR-21. The cut points correspond to the maximum Chi-square value of the Kaplan-Meier test for OS between groups above and below the cut-point threshold. p85 $\alpha$  downregulation was found in 25 (7.8%) of the 320 breast cancer

patients. miR-21 high expression was found in 119 (37.2%) of 320 patients. Next, we investigated the negative regulation of endogenous p85 $\alpha$  protein by endogenous miR-21. Correlation analysis demonstrated that endogenous p85 $\alpha$  protein levels were not statistically correlated with miR-21 in the patient tumor specimens (Fig. 5C; rs=-0.109, P=0.052, Spearman's correlation analysis).

*Correlation of p85 $\alpha$  expression with breast cancer clinicopathological characteristics and prognosis.* p85 $\alpha$  downregulation was associated with PR positive status (Table IV; P=0.047). No significant correlation was observed between p85 $\alpha$  and

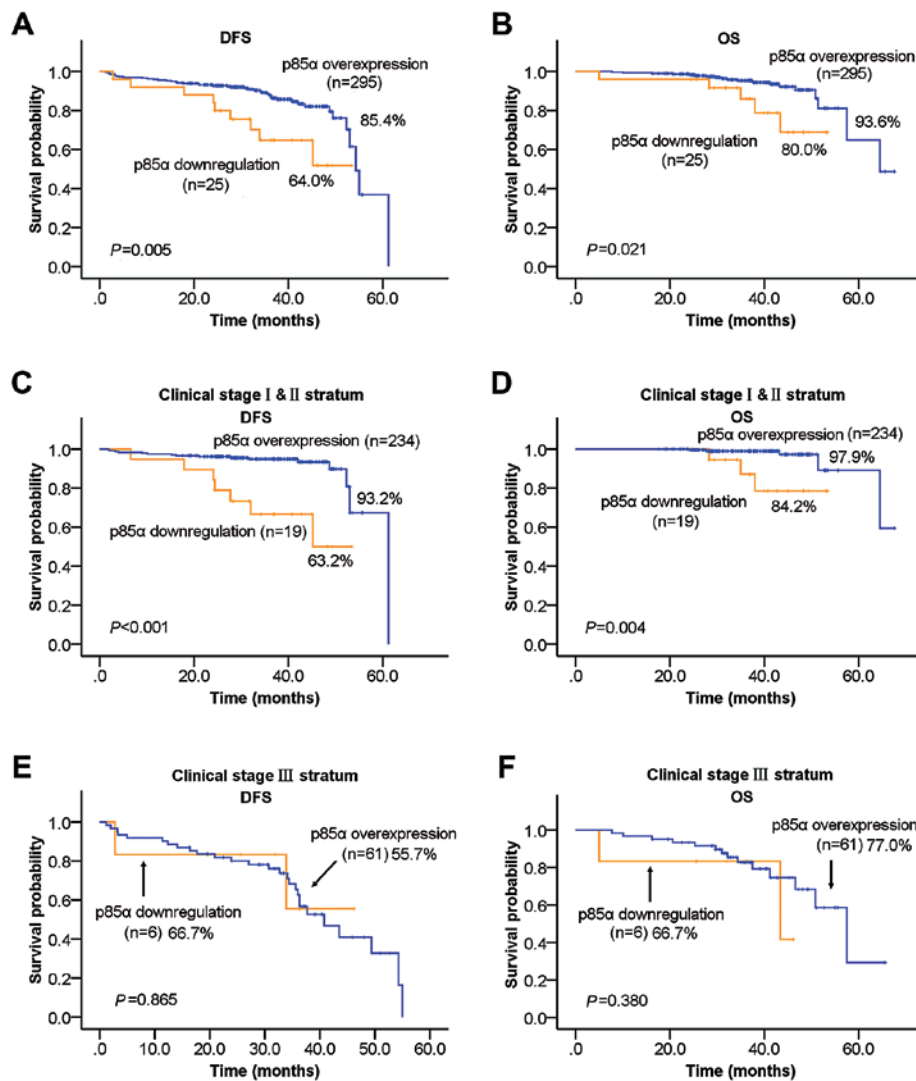


Figure 6. Prognostic impact of p85α protein expression in breast cancer patients. Kaplan-Meier estimates of (A) 5-year DFS and (B) 5-year OS for all patients with p85α overexpression or downregulation. Kaplan-Meier estimates of (C) 5-year DFS and (D) 5-year OS for patients with clinical stage I and II breast cancer. Kaplan-Meier estimates of (E) 5-year DFS and (F) 5-year OS for patients with clinical stage III breast cancer. OS, overall survival; DFS, disease-free survival.

clinical stage, tumor size, node status, histological grade, ER or HER2 status. miR-21 overexpression was associated with high clinical stage (Table IV;  $P=0.016$ ). No correlation was observed between miR-21 and other characteristic.

Next, we investigated the prognostic impact of p85α and miR-21 expression on breast cancer patients. The survival curves showed that p85α downregulation was significantly associated with inferior 5-year DFS and OS of breast cancer patients (Fig. 6A and B; DFS:  $P=0.005$ , OS:  $P=0.021$ ; log-rank tests). Within early stage stratum, patients with p85α downregulation had inferior 5-year DFS and OS compared to those with p85α overexpression (Fig. 6C and D;  $P<0.001$  for DFS,  $P=0.004$  for OS, log-rank test). However, within the late stage stratum, p85α expression was not related with the patient survival (Fig. 6E and F). Consistent with our previous study in another cohort, high miR-21 expression was significantly associated with inferior 5-year DFS and 5-year OS in this cohort (DFS:  $P=0.035$ ; OS,  $P=0.028$ ).

In univariate analysis, p85α downregulation, high miR-21, high clinical stage, tumor size >2 cm, node positive,

high histological grade and breast conservation were associated with inferior 5-year DFS and 5-year OS of the breast cancer patients (Table V). While, subtypes of breast cancer, hormone receptor status, HER2 status, and chemotherapy were not associated with inferior 5-year DFS or 5-year OS. Multivariate Cox regression model that incorporated significant factors in the univariate analyses showed that only p85α downregulation and high clinical stage maintained independent prognostic factors for both inferior 5-year OS and DFS (Table VI).

## Discussion

In the present study, we present evidence that *PIK3R1* is a direct miR-21 target. *PIK3R1* phenocopies the effect of miR-21 knockdown. Furthermore, we expanded our previous findings that miR-21 knockdown suppresses cell growth, migration and invasion by inhibiting PI3K/AKT activation via targeting *PIK3R1*. AntimiR-21/*PIK3R1*-induced suppression of invasiveness in breast cancer cells is mediated by reversing

Table V. Univariate Cox models for patients with invasive breast cancer.

Characteristics	OS			DFS		
	HR	95% CI	P	HR	95% CI	P-value
p85 $\alpha$ overexpression vs. downregulation	3.06	1.13-8.31	0.028	2.68	1.30-5.54	0.008
miR-21 low vs. high	2.47	1.08-5.65	0.033	1.80	1.03-3.12	0.038
Clinical stage I vs. II vs. III	4.20	2.15-8.20	<0.001	3.59	2.35-5.50	<0.001
Tumor size (cm) $\leq 2$ vs. $>2$	3.44	1.28-9.27	0.015	3.82	1.95-7.46	<0.001
Node negative vs. positive	5.38	2.00-14.45	0.001	3.76	2.02-6.98	<0.001
Histological grade 1 vs. 2 vs. 3	2.57	1.19-5.55	0.017	2.25	1.47-3.45	<0.001
Subtypes of breast cancer	1.25	0.77-2.04	0.371	1.01	0.72-1.43	0.944
ER negative vs. positive	0.63	0.25-1.59	0.327	0.95	0.46-1.97	0.891
PR negative vs. positive	0.96	0.36-2.58	0.933	1.19	0.57-2.46	0.646
HER2 negative vs. positive	0.70	0.20-2.39	0.577	0.99	0.48-2.07	0.991
Mastectomy vs. breast conservation	0.50	0.26-0.95	0.033	0.63	0.42-0.95	0.026
Neoadjuvant chemotherapy vs. adjuvant chemotherapy vs. not given	0.33	0.05-2.48	0.282	0.55	0.20-1.52	0.246

Italics indicate significance. <sup>a</sup>Sample sizes differ due to complete data set per Cox model.

Table VI. Multivariate Cox model for patients with invasive breast cancer.

Characteristics	5-year OS			5-year DFS		
	HR	95% CI	P-value <sup>a</sup>	HR	95% CI	P-value <sup>a</sup>
p85 $\alpha$ overexpression vs. downregulation	3.42	1.24-9.41	0.017	2.90	1.39-6.04	0.004
Clinical stage I vs. II vs. III	4.59	2.27-9.31	<0.001	3.34	2.19-5.10	<0.001

Italics indicate significance. <sup>a</sup>Cox regression forward LR method.

EMT. Additionally, we show an inverse correlation between p85 $\alpha$  expression levels and PR expression in patient tumors. Finally, we demonstrate that p85 $\alpha$  is downregulated in patients with invasive breast cancer, indicating an inferior prognosis. Taken together, our data provide novel insight into the regulation of p85 $\alpha$  expression in breast cancer and its potential role on prognosis predication.

miR-21 is an oncomiR in breast cancer and targets several tumor suppressor genes important for various cellular processes (22). Here, we show that p85 $\alpha$  is downregulated in 7.8% of breast cancer tumors, and is a direct target of miR-21. This finding is consistent with a recent study by Toste *et al* (32). They demonstrated a direct regulation of p85 $\alpha$  by miR-21 and an inverse correlation between miR-21 and p85 $\alpha$  expression levels in human pancreatic tumors. However, we did not find a statistically significant correlation between miR-21 and p85 $\alpha$  expression levels in patient tumors (P=0.052). We speculate that patient tumor sections for quantitative detection of miR-21, which inevitably contain both normal and malignant cells, are the most possible reason for this inconsistent result.

The protein p85 $\alpha$  is necessary for stabilization and membrane recruitment of the p110 $\alpha$  subunit of PI3K (6). Loss of the p85 $\alpha$  protein leads to downstream PI3K pathway activation (30,32-35). Therefore, the impact of p85 $\alpha$  down-

regulation on pathway signaling could be caused by the loss of the inhibitory effect of p85 $\alpha$  on p110 $\alpha$  and PI3K pathway activity (33,36). p85 $\alpha$  protein has also been reported to be a positive regulator of PTEN via stabilization of this protein (37,38). Besides, several studies evidenced that PTEN is one of miR-21 targets (21,38,39). These studies support the notion that miR-21 activates PI3K pathway via multiple targets. Our finding that p-AKT levels are decreased after p85 $\alpha$  overexpression in breast cancer cells is consistent with these previous observations. In addition, PIK3R1 overexpression phenocopies the effect of miR-21 knockdown on breast cancer cells and PIK3R1 knockdown inversely abrogates LNA-antimiR-21-mediated cell growth and invasion suppression. These findings suggest that PIK3R1 exerts tumor suppressor properties in breast cancer. Furthermore, the concept that p85 $\alpha$  downregulation can be protumorigenic (30) is supported by our finding that p85 $\alpha$  downregulation is seen in breast cancer tissues when compared with normal tissues. In the present study, this newly identified p85 $\alpha$  downregulation by miR-21 has significant importance for interpretation of miR-21 promoting breast cancer cells growth, migration and invasion through the PI3K/AKT pathway.

Prognosis of invasive breast cancer, no special type, is influenced by the classical variables of histological grade,



tumor size, lymph node status and clinical stage (14,29,40,41). However, heterogeneity in tumor cell phenotypes make breast tumor categorization a challenging task, especially as it is relevant to therapeutic responses and patient prognosis (1). Our previous study and other research demonstrated that elevated miR-21 could predict unfavorable prognosis in breast cancer patients (23,42-44). In this study, we performed an evaluation of the prognostic significance of p85 $\alpha$ , as well as miR-21, in a 320 patient cohort, and confirmed that miR-21 was a prognostic marker for inferior 5-year DFS and 5-year OS in breast cancer patients. Noticeably, p85 $\alpha$  downregulation was a prognostic marker for inferior clinical stage. This finding is consistent with the association between p85 $\alpha$  downregulation and an inferior prognosis not only in breast cancer (15) but also pancreatic cancer (32,45), hepatocellular cancers (30), neuroblastoma (46) and lung cancers (47). All these results support the notion that p85 $\alpha$  plays as a tumor suppressor gene in invasive breast cancer tumors. Additional *in vivo* studies will be necessary to confirm the relationship between miR-21 and p85 $\alpha$ , and the role of p85 $\alpha$  in breast cancer.

In conclusion, we provided evidence that *PIK3R1* is a direct target of miR-21. miR-21 knockdown induced increased p85 $\alpha$  level, accompanied by decreased p-AKT level. miR-21 may play a role in breast cancer development by promoting breast cancer cell growth, migration and invasion partly by inhibiting PI3K/AKT activation via targeting *PIK3R1* and reversing EMT. Furthermore, alterations in miR-21 and p85 $\alpha$  had a complementary impact on breast cancer patient survival. Finally, p85 $\alpha$  downregulation defined a specific subgroup of breast cancer with shorter 5-year DFS and OS, which may require more aggressive treatment.

### Acknowledgements

We thank Xin-Chuang Cai and Jia Fu for support with TMAs construction and IHC staining. The present study was funded by the National Natural Science Foundation of China (NSFC, <http://www.nsf.gov.cn/>) (grant nos. 81202111 and 81302143), the Guangdong Natural Science Foundation (grant no. S2012040006409), and a National Clinical Key Subject Construction Project Foundation of China. All procedures performed in studies involving human participants were in accordance with the ethical standards of the institutional and national research committee and with the 1964 Helsinki declaration and its later amendments or comparable ethical standards. This research involved formalin-fixed paraffin-embedded tissue specimens from breast cancer patients. For retrospective studies formal consent was not required.

### References

- Polyak K: Heterogeneity in breast cancer. *J Clin Invest* 121: 3786-3788, 2011.
- Banerji S, Cibulskis K, Rangel-Escareno C, Brown KK, Carter SL, Frederick AM, Lawrence MS, Sivachenko AY, Sougnez C, Zou L, *et al*: Sequence analysis of mutations and translocations across breast cancer subtypes. *Nature* 486: 405-409, 2012.
- Goldhirsch A, Winer EP, Coates AS, Gelber RD, Piccart-Gebhart M, Thürlimann B, Senn HJ, Albain KS, Andre F, Bergh J, *et al*: Panel members: Personalizing the treatment of women with early breast cancer: Highlights of the St Gallen International Expert Consensus on the Primary Therapy of Early Breast Cancer 2013. *Ann Oncol* 24: 2206-2223, 2013.
- Elkabets M, Vora S, Juric D, Morse N, Mino-Kenudson M, Muranen T, Tao J, Campos AB, Rodon J, Ibrahim YH, *et al*: mTORC1 inhibition is required for sensitivity to PI3K p110 $\alpha$  inhibitors in PIK3CA-mutant breast cancer. *Sci Transl Med* 5: 196ra99, 2013.
- Myhre S, Lingjærde OC, Hennessy BT, Aure MR, Carey MS, Alsnér J, Tramm T, Overgaard J, Mills GB, Børresen-Dale AL, *et al*: Influence of DNA copy number and mRNA levels on the expression of breast cancer related proteins. *Mol Oncol* 7: 704-718, 2013.
- Yuan TL and Cantley LC: PI3K pathway alterations in cancer: Variations on a theme. *Oncogene* 27: 5497-5510, 2008.
- Uchino M, Kojima H, Wada K, Imada M, Onoda F, Satofuka H, Utsugi T and Murakami Y: Nuclear beta-catenin and CD44 upregulation characterize invasive cell populations in non-aggressive MCF-7 breast cancer cells. *BMC Cancer* 10: 414, 2010.
- Engelman JA: Targeting PI3K signalling in cancer: Opportunities, challenges and limitations. *Nat Rev Cancer* 9: 550-562, 2009.
- Hennessy BT, Smith DL, Ram PT, Lu Y and Mills GB: Exploiting the PI3K/AKT pathway for cancer drug discovery. *Nat Rev Drug Discov* 4: 988-1004, 2005.
- Zhao L and Vogt PK: Class I PI3K in oncogenic cellular transformation. *Oncogene* 27: 5486-5496, 2008.
- Juric D, Castel P, Griffith M, Griffith OL, Won HH, Ellis H, Ebbesen SH, Ainscough BJ, Ramu A, Iyer G, *et al*: Convergent loss of PTEN leads to clinical resistance to a PI(3)K $\alpha$  inhibitor. *Nature* 518: 240-244, 2015.
- Brachmann SM, Ueki K, Engelman JA, Kahn RC and Cantley LC: Phosphoinositide 3-kinase catalytic subunit deletion and regulatory subunit deletion have opposite effects on insulin sensitivity in mice. *Mol Cell Biol* 25: 1596-1607, 2005.
- Zhao L and Vogt PK: Helical domain and kinase domain mutations in p110 $\alpha$  of phosphatidylinositol 3-kinase induce gain of function by different mechanisms. *Proc Natl Acad Sci USA* 105: 2652-2657, 2008.
- Araújo TG, Paiva CE, Rocha RM, Maia YC, Sena AA, Ueira-Vieira C, Carneiro AP, Almeida JF, de Faria PR, Santos DW, *et al*: A novel highly reactive Fab antibody for breast cancer tissue diagnostics and staging also discriminates a subset of good prognostic triple-negative breast cancers. *Cancer Lett* 343: 275-285, 2014.
- Cizkova M, Vacher S, Meseure D, Trassard M, Susini A, Mlcuchova D, Callens C, Rouleau E, Spyrtos F, Lidereau R, *et al*: PIK3R1 underexpression is an independent prognostic marker in breast cancer. *BMC Cancer* 13: 545, 2013.
- Visani M, de Biase D, Marucci G, Cerasoli S, Nigrisoli E, Bacchi Reggiani ML, Albani F, Baruzzi A and Pession A; PERNO study group: Expression of 19 microRNAs in glioblastoma and comparison with other brain neoplasia of grades I-III. *Mol Oncol* 8: 417-430, 2014.
- Jamali Z, Asl Aminabadi N, Attaran R, Pournagiazar F, Ghertasi Oskouei S and Ahmadpour F: MicroRNAs as prognostic molecular signatures in human head and neck squamous cell carcinoma: A systematic review and meta-analysis. *Oral Oncol* 51: 321-331, 2015.
- Zhang F, Yang Z, Cao M, Xu Y, Li J, Chen X, Gao Z, Xin J, Zhou S, Zhou Z, *et al*: MiR-203 suppresses tumor growth and invasion and down-regulates MiR-21 expression through repressing Ran in esophageal cancer. *Cancer Lett* 342: 121-129, 2014.
- Abue M, Yokoyama M, Shibuya R, Tamai K, Yamaguchi K, Sato I, Tanaka N, Hamada S, Shimosegawa T, Sugamura K, *et al*: Circulating miR-483-3p and miR-21 is highly expressed in plasma of pancreatic cancer. *Int J Oncol* 46: 539-547, 2015.
- Shi Z, Zhang J, Qian X, Han L, Zhang K, Chen L, Liu J, Ren Y, Yang M, Zhang A, *et al*: AC1MMYR2, an inhibitor of dicer-mediated biogenesis of Oncomir miR-21, reverses epithelial-mesenchymal transition and suppresses tumor growth and progression. *Cancer Res* 73: 5519-5531, 2013.
- Li LQ, Li XL, Wang L, Du WJ, Guo R, Liang HH, Liu X, Liang DS, Lu YJ, Shan HL, *et al*: Matriline inhibits breast cancer growth via miR-21/PTEN/Akt pathway in MCF-7 cells. *Cell Physiol Biochem* 30: 631-641, 2012.
- Baffa R, Fassan M, Volinia S, O'Hara B, Liu CG, Palazzo JP, Gardiman M, Rugge M, Gomella LG, Croce CM, *et al*: MicroRNA expression profiling of human metastatic cancers identifies cancer gene targets. *J Pathol* 219: 214-221, 2009.



23. Yan LX, Huang XF, Shao Q, Huang MY, Deng L, Wu QL, Zeng YX and Shao JY: MicroRNA miR-21 overexpression in human breast cancer is associated with advanced clinical stage, lymph node metastasis and patient poor prognosis. *RNA* 14: 2348-2360, 2008.
24. Yan LX, Wu QN, Zhang Y, Li YY, Liao DZ, Hou JH, Fu J, Zeng MS, Yun JP, Wu QL, *et al*: Knockdown of miR-21 in human breast cancer cell lines inhibits proliferation, in vitro migration and in vivo tumor growth. *Breast Cancer Res* 13: R2, 2011.
25. Gramantieri L, Ferracin M, Fornari F, Veronese A, Sabbioni S, Liu CG, Calin GA, Giovannini C, Ferrazzi E, Grazi GL, *et al*: Cyclin G1 is a target of miR-122a, a microRNA frequently down-regulated in human hepatocellular carcinoma. *Cancer Res* 67: 6092-6099, 2007.
26. Gao L, Song JR, Zhang JW, Zhao X, Zhao QD, Sun K, Deng WJ, Li R, Lv G, Cheng HY, *et al*: Chloroquine promotes the anticancer effect of TACE in a rabbit VX2 liver tumor model. *Int J Biol Sci* 9: 322-330, 2013.
27. Sun L, Li H, Chen J, Dehennaut V, Zhao Y, Yang Y, Iwasaki Y, Kahn-Perles B, Leprince D, Chen Q, *et al*: A SUMOylation-dependent pathway regulates SIRT1 transcription and lung cancer metastasis. *J Natl Cancer Inst* 105: 887-898, 2013.
28. De Bacco F, Luraghi P, Medico E, Reato G, Girolami F, Perera T, Gabriele P, Comoglio PM and Boccaccio C: Induction of MET by ionizing radiation and its role in radioresistance and invasive growth of cancer. *J Natl Cancer Inst* 103: 645-661, 2011.
29. Sunil RL, Lan OE, Stuart JS, Puay HT and Marc JV: WHO Classification of Tumours. Fred TB, Elain SJ, Sunil RL and Hiroko O (eds). IARC Press, Lyon, pp240, 2012.
30. Taniguchi CM, Winnay J, Kondo T, Bronson RT, Guimaraes AR, Alemán JO, Luo J, Stephanopoulos G, Weissleder R, Cantley LC, *et al*: The phosphoinositide 3-kinase regulatory subunit p85alpha can exert tumor suppressor properties through negative regulation of growth factor signaling. *Cancer Res* 70: 5305-5315, 2010.
31. Richardson AL, Wang ZC, De Nicolo A, Lu X, Brown M, Miron A, Liao X, Iglehart JD, Livingston DM and Ganesan S: X chromosomal abnormalities in basal-like human breast cancer. *Cancer Cell* 9: 121-132, 2006.
32. Toste PA, Li L, Kadera BE, Nguyen AH, Tran LM, Wu N, Madnick DL, Patel SG, Dawson DW and Donahue TR: p85 $\alpha$  is a microRNA target and affects chemosensitivity in pancreatic cancer. *J Surg Res* 196: 285-293, 2015.
33. Shekar SC, Wu H, Fu Z, Yip SC, Nagajyothi, Cahill SM, Girvin ME and Backer JM: Mechanism of constitutive phosphoinositide 3-kinase activation by oncogenic mutants of the p85 regulatory subunit. *J Biol Chem* 280: 27850-27855, 2005.
34. Luo J and Cantley LC: The negative regulation of phosphoinositide 3-kinase signaling by p85 and its implication in cancer. *Cell Cycle* 4: 1309-1312, 2005.
35. Rabinovsky R, Pochanard P, McNear C, Brachmann SM, Duke-Cohan JS, Garraway LA and Sellers WR: p85 associates with unphosphorylated PTEN and the PTEN-associated complex. *Mol Cell Biol* 29: 5377-5388, 2009.
36. Jaiswal BS, Janakiraman V, Kljavin NM, Chaudhuri S, Stern HM, Wang W, Kan Z, Dbouk HA, Peters BA, Waring P, *et al*: Somatic mutations in p85alpha promote tumorigenesis through class IA PI3K activation. *Cancer Cell* 16: 463-474, 2009.
37. Cheung LW, Hennessy BT, Li J, Yu S, Myers AP, Djordjevic B, Lu Y, Stemke-Hale K, Dyer MD, Zhang F, *et al*: High frequency of PIK3R1 and PIK3R2 mutations in endometrial cancer elucidates a novel mechanism for regulation of PTEN protein stability. *Cancer Discov* 1: 170-185, 2011.
38. Darido C, Georgy SR, Wilanowski T, Dworkin S, Auden A, Zhao Q, Rank G, Srivastava S, Finlay MJ, Papenfuss AT, *et al*: Targeting of the tumor suppressor GRHL3 by a miR-21-dependent proto-oncogenic network results in PTEN loss and tumorigenesis. *Cancer Cell* 20: 635-648, 2011.
39. Xiong B, Cheng Y, Ma L and Zhang C: MiR-21 regulates biological behavior through the PTEN/PI-3 K/Akt signaling pathway in human colorectal cancer cells. *Int J Oncol* 42: 219-228, 2013.
40. Badwe R, Hawaldar R, Parmar V, Nadkarni M, Shet T, Desai S, Gupta S, Jalali R, Vanmali V, Dikshit R, *et al*: Single-injection depot progesterone before surgery and survival in women with operable breast cancer: A randomized controlled trial. *J Clin Oncol* 29: 2845-2851, 2011.
41. Uji K, Naoi Y, Kagara N, Shimoda M, Shimomura A, Maruyama N, Shimazu K, Kim SJ and Noguchi S: Significance of TP53 mutations determined by next-generation 'deep' sequencing in prognosis of estrogen receptor-positive breast cancer. *Cancer Lett* 342: 19-26, 2014.
42. Müller V, Gade S, Steinbach B, Loibl S, von Minckwitz G, Untch M, Schwedler K, Lübke K, Schem C, Fasching PA, *et al*: Changes in serum levels of miR-21, miR-210, and miR-373 in HER2-positive breast cancer patients undergoing neoadjuvant therapy: A translational research project within the Geparquinto trial. *Breast Cancer Res Treat* 147: 61-68, 2014.
43. Markou A, Yousef GM, Stathopoulos E, Georgoulas V and Lianidou E: Prognostic significance of metastasis-related microRNAs in early breast cancer patients with a long follow-up. *Clin Chem* 60: 197-205, 2014.
44. Lee JA, Lee HY, Lee ES, Kim I and Bae JW: Prognostic implications of MicroRNA-21 overexpression in invasive ductal carcinomas of the breast. *J Breast Cancer* 14: 269-275, 2011.
45. Donahue TR, Tran LM, Hill R, Li Y, Kovoichich A, Calvopina JH, Patel SG, Wu N, Hindoyan A, Farrell JJ, *et al*: Integrative survival-based molecular profiling of human pancreatic cancer. *Clin Cancer Res* 18: 1352-1363, 2012.
46. Fransson S, Abel F, Kogner P, Martinsson T and Ejeskär K: Stage-dependent expression of PI3K/Akt-pathway genes in neuroblastoma. *Int J Oncol* 42: 609-616, 2013.
47. Lu Y, Lemon W, Liu PY, Yi Y, Morrison C, Yang P, Sun Z, Szoke J, Gerald WL, Watson M, *et al*: A gene expression signature predicts survival of patients with stage I non-small cell lung cancer. *PLoS Med* 3: e467, 2006.